Article

Spontaneous Self-Assembly of Silica Nanocages into Inorganic Framework Materials

N. Ning, F. Calvo, A. C. T. van Duin, D. J. Wales, and H. Vach

J. Phys. Chem. C, **2009**, 113 (2), 518-523 • Publication Date (Web): 17 December 2008

Spontaneous Self-Assembly of Silica Nanocages into Inorganic Framework Materials

N. Ning

LPICM, Ecole Polytechnique, CNRS, 91128, Palaiseau, France

F. Calvo*

LASIM, Université de Lyon, Bât. A. Kastler, 43 Bd du 11 novembre 1918, F69622 Villeurbanne Cedex, France

A. C. T. van Duin

Material and Process Simulation Center, California Institute of Technology, Pasadena, California 91125

D. J. Wales

University Chemical Laboratories, Lensfield Road, Cambridge CB2 1EW, United Kingdom

H. Vach

LPICM, Ecole Polytechnique, CNRS, 91128, Palaiseau, France

Received: May 22, 2008; Revised Manuscript Received: October 13, 2008

The possibility of the formation of different silica nanostructures based on fully coordinated spheroidal nanocages $(SiO_2)_{24}$ is theoretically investigated using a pairwise potential and the $ReaxFF_{SiO}$ reactive force field. Molecular dynamics simulations at $T = 300$ K predict that while these nanocages are thermally stable, they spontaneously undergo dimerization upon contact by forming two siloxane bridges. The corresponding reaction pathways obtained with both methods are quantitatively confirmed by electronic structure calculations performed at the Hartree-Fock and density functional theory levels. The barrierless dimerization of silica nanocages is the first step of subsequent polymerizations into strongly bound inorganic materials. Routes to polymerization and possible applications are discussed.

I. Introduction

Silica-based nanostructured materials are widely used for their optical and electronic properties in sensing devices, microelectronics, communication, thin film devices, and bionanotechnological applications.[1−4] Silica nanoparticles also play a key role in adsorption, ion exchange, and catalytic processes.[5,6] The observed enhancement of electronic, optical, and catalytic properties is due to the higher surface/volume ratio of the nanoparticles over bulk materials and to the dramatic role played by their surface structure.[7] Exploiting the advantages of silica nanoparticles over conventional bulk materials could be achieved through periodic arrays of clusters. Such crystalline assemblies would thus form a nanoporous silica network, similar in many respects to zeolites. As noted by Bromley,[8] building nanoporous silica assemblies from nanoparticles faces two main challenges. First, the individual clusters need to be synthesized in large amounts with control over their shape, which requires not only perfect size selection but also stringent control of morphology. Second, these clusters should be stable thermodynamically, and they should not coalesce with each other. This condition is usually not met for metal nanoparticles unless they are surrounded by passivating ligands, but it is obviously necessary for the successful self-assembly of framework materials.

With the rapid progress in experimental techniques used for nanocluster formation, which include plasma discharge, flame oxidation, and laser ablation, we anticipate that the ability to control the size and structure for nanoparticles will continue to improve. Theory and modeling can contribute to this effort by elucidating possible structural candidates. The stable structures of silica nanoclusters $(SiO_2)_n$ have been theoretically investigated by several groups,[9−24] at levels ranging from analytic pair potentials to density functional theory (DFT) calculations. These studies suggest that fully coordinated structures are particularly stable with respect to lower dimensional chain or ring geometries.[16] Even though they may not be the most stable for a given size,[19] fully coordinated spheroidal nanocages are generally expected to be lower in energy than elongated, nanotube-like structures.[6]

Complete coordination of surface atoms seems to be a necessary condition for the stability of silica nanoclusters against coalescence. Stable packings of such fully coordinated clusters, particularly rings and cages, have been recently proposed by Bromley who obtained low density molecular materials by DFT local minimization.[8] Using the TTAM pair potential,[25] Schweigert and co-workers[26] found from molecular dynamics simulations that medium sized clusters containing several hundreds of SiO_2 units spontaneously melt and coalesce at high temperatures $T > 1500$ K.

In the present work, we have examined the stability of $(SiO_2)_{24}$ silica nanocages with respect to coalescence using a variety of theoretical methods. The Flikkema−Bromley (FB) analytical potential[27] is computationally cheap and allows a straightforward exploration of the reactivity of silica nanocages, including some kinetic aspects. The multibody ReaxFF reactive

10.1021/jp804528z CCC: $40.75
Published on Web 12/17/2008

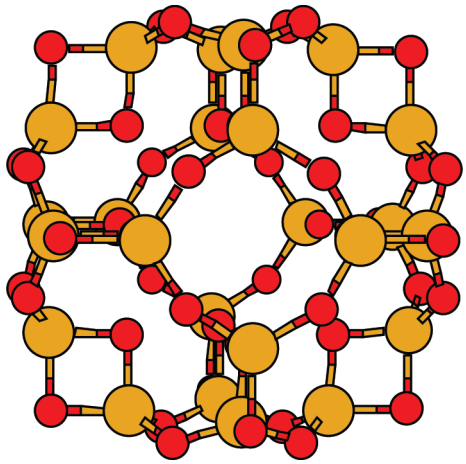

Figure 1. Fully coordinated $(SiO_2)_{24}$ nanocluster in an octahedral configuration.

force field,[28,29] while also based on explicit (but far more involved) interactions, provides a more realistic approach, albeit still within a dynamical framework. Lastly, we used DFT and Hartree-Fock calculations to validate the FB and ReaxFF methods for the $(SiO_2)_{24}$ dimerization reaction and subsequently employed the FB and ReaxFF methods, which are orders of magnitudes faster than quantum mechanical (QM) methods, to simulate the interaction of multiple SiO_2 nanocages using molecular dynamics simulations. This combined approach provides a quantitative assessment of the stability of the silica nanocages. Our simulations indicate that, although they are fully coordinated, the $(SiO_2)_{24}$ nanoclusters undergo spontaneous dimerization and polymerization reactions under ambient conditions. This mechanism leads to the formation of inorganic frameworks in which the individual clusters are linked together by Si−O−Si siloxane bridges.

The present article is organized as follows. The next section is devoted to the molecular simulations carried out using the FB potential and ReaxFF. The dimerization pathways are discussed first in the light of these models, and then studied in section III with explicit treatment of the electronic structure. In section IV we discuss the formation of assemblies larger than the dimer, as the first step toward nanoporous materials. Finally, in section V we draw some overall conclusions.

II. Molecular Simulations

The silica nanocage $(SiO_2)_{24}$ first proposed in ref 16 is fully coordinated and has octahedral symmetry, making it a good candidate for self-assembly into a variety of materials (Figure 1). While it may not be the lowest energy structure at this size,[19] the octahedral cage is appealing due to its hollow morphology. This feature was noted earlier by LaViolette and Benson, who investigated a series of highly symmetric fullerene-like hydrides and oxides of various elements including boron, carbon, and silicon.[30]

A. Pair Potential. We start our exploration of the interaction between silica nanocages by performing explicit molecular dynamics simulations using a simple pair potential fitted to reproduce the energetic properties of SiO_2 clusters. Similar to the TTAM[25] and BKS[31] models, the Flikkema−Bromley (FB) potential is based on a Buckingham expression for the pair interaction, supplemented by a Coulomb term

$$E_{ij} = A_{ij}\exp\left(-\frac{r_{ij}}{B_{ij}}\right) + \chi(r_{ij})\left[-\frac{C_{ij}}{r_{ij}^{6}} + \frac{q_i q_j}{r_{ij}}\right] \qquad (1)$$

In the above expression, r_{ij} is the distance between atoms i and j, q_i is the partial charge carried by atom i, and A_{ij}, B_{ij}, and C_{ij} are parameters fitted to reproduce DFT results obtained at the B3LYP/6-31G* level.[27] In order to avoid possible problems at short distances arising from the strongly attractive dispersion interaction, the last two terms of the potential were shielded using a standard cutoff function, $\chi(r_{ij})$, given by

$$\chi(r_{ij}) = \begin{cases} \exp[-(1 - R_{ij}/r_{ij})^2], & \text{if } r_{ij} < R_{ij} \\ 1, & \text{if } r_{ij} \geq R_{ij} \end{cases} \qquad (2)$$

The cutoff parameters were chosen as $R_{SiSi} = 1.27$ Å, $R_{OO} = 1.5$ Å, and $R_{SiO} = 1.2$ Å.

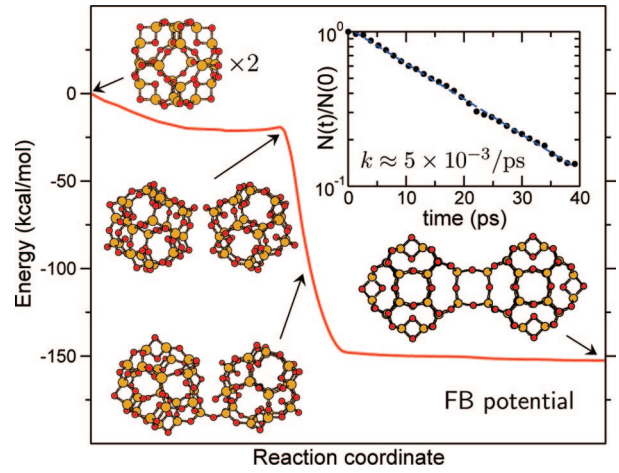

Figure 2. Reaction pathway for the $(SiO_2)_{24}$ dimerization obtained with the FB pair potential. The inset shows the evolution of the number of $(SiO_2)_{24}$ units that have not reacted yet as a function of time after first contact in molecular dynamics simulations at 300 K.

Molecular dynamics simulations of the individual $(SiO_2)_{24}$ cluster were performed at increasing temperatures using the velocity Verlet algorithm with a time step of 1.3 fs. The individual nanocage was found to be stable against melting up to about 1500 K, in agreement with the results by Schweigert and co-workers.[26] Simulations of soft collisions were then carried out by thermalizing two clusters separately at 300 K, placing them at a distance of 24 Å, and varying the impact parameter randomly between 0 and 4 Å. For each simulation, the initial orientations of the two clusters were randomly distributed. After 10 ps of equilibration at 300 K, the clusters were given relative velocities toward each other corresponding to 300 K of translational kinetic energy. Upon contact, the two clusters initially undergo a soft bouncing followed by rotational motion around the common center of mass. This rotational motion is followed after a few tens of picoseconds by a spontaneous reaction in which two nearby Si−O bonds from each cluster break, the oxygen atoms move to form bridging siloxane bonds between the clusters, and a stable dimer results. (A typical trajectory is displayed as Supporting Information.)

When the number of clusters that have not yet formed a dimer is monitored as a function of time t after contact, $N(t)$, the dimerization rate constant may be determined by a linear fit of $N(t)/N(t = 0)$ on a logarithmic scale. The variations of $N(t)/N(0)$ obtained from 10^4 independent trajectories are shown in the inset of Figure 2 as a function of time. The rate constant is estimated to be about 2×10^{-5} ps^{-1}, indicating that the reaction between two $(SiO_2)_{24}$ nanocages occurs very quickly under mild conditions with the FB potential.

The dimerization pathway was calculated for the present reaction using the doubly[32] nudged elastic band method,[33,34] as implemented in the OPTIM code.[33] The energy profile of the pathway, shown in Figure 2, reveals a single-step mechanism

in which the two nanocages first rotate, thus bringing two oxygens from Si_2O_2 rhombi within 2 Å. One siloxane bond breaks, leaving one dangling oxygen atom and a silicon atom only 3-fold coordinated. Very quickly, the facing siloxane bond also breaks, the oxygen atom connects with the undercoordinated silicon atom of the other cage, and the previously dangling oxygen connects with the newly formed undercoordinated silicon.

The final configuration obtained from this dimerization reaction binds the two nanocages by two siloxane bridges. This dimer is quite flexible around the newly formed bonds, but it is a true minimum on the potential energy surface. Interestingly, the only local barrier to dimerization is very small (a few kcal/mol) and corresponds to a reorientation of the clusters. The overall gain in binding energy for this reaction is −152.52 kcal/mol for the FB potential.

We have also attempted to simulate the dimerization of two $(SiO_2)_{24}$ nanocages using the BKS and TTAM parametrizations of the pair potential. Both models were found to be even more reactive than the FB potential, often leading to limited coalescence, with a partial loss of the initial octahedral geometry. For these two potentials, the dimer bound by two planar siloxane bridges is not a minimum, but a saddle point of index 4.

B. Reax Force Field. The simulation of silica nanocages over several hundreds of nanoseconds with meaningful statistics is only feasible with simple analytical potentials such as the FB model. A chemically more realistic description of the dimerization between fully coordinated $(SiO_2)_{24}$ clusters is offered by the many-body ReaxFF force field[28] extended for Si−O−H interactions.[29] Briefly, the energy surface in the $ReaxFF_{SiO}$ model is built from the sum of several contributions,

$$E_{total} = E_{bond} + E_{over} + E_{under} + E_{lp} + E_{val} + E_{pen} + E_{tors} + E_{conj} + E_{vdW} + E_{Coulomb} \quad (3)$$

The various terms in the above equation account for the bond energy, valence and torsion angles, van der Waals and Coulomb energies, as well as corrections for over- and undercoordination. The full details and expressions are given in ref 29.

Molecular dynamics simulations of the thermal stability of $(SiO_2)_{24}$ nanocages and of the reaction between two $(SiO_2)_{24}$ clusters have been performed with the $ReaxFF_{SiO}$ model, using bond restraints to drive the dimerization. Using this method, we find that the nanocage remains stable up to a temperature of 300 K, while it starts to deform slightly at 400 K. The dimerization simulations were initialized by giving vibrational and translational energy to each cluster corresponding to a low temperature of 5 K, in order to provide a suitable comparison with the 0 K potential energy pathway of Figure 2. The reaction between the nanocages again occurs through breaking of two Si−O bonds and the consecutive formation of two siloxane bridges between the cages, as illustrated in Figure 3.

The $ReaxFF_{SiO}$ pathway is very similar to the FB pathway. The small energy barrier on the ReaxFF pathway is related to the sliding restraint method used in the ReaxFF program to track reaction coordinates and does not constitute a formal transition state. The atomistic mechanism for dimerization differs slightly from the pathway obtained with the pair potential and involves the simultaneous breaking of Si−O bonds from facing Si_2O_2 rhombi, followed by the pivoting of the dangling oxygens to the opposite silicon atoms left undercoordinated. The rate-limiting step, highlighted in Figure 3, consists of the initial formation of the two siloxane bridges, after which the two cages rotate to optimize this bridging interaction.

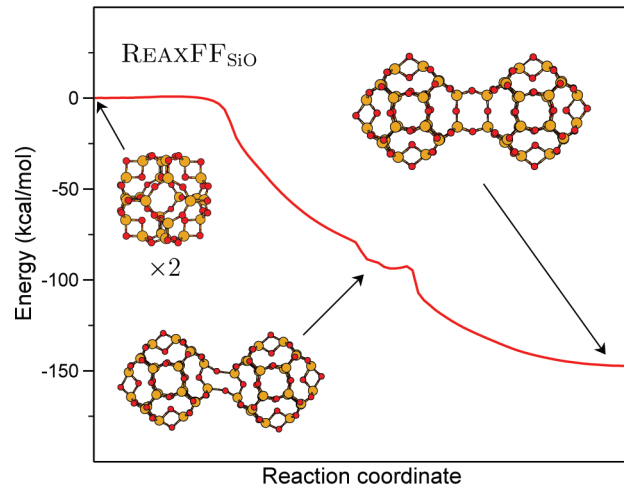

Figure 3. Reaction pathway for the $(SiO_2)_{24}$ dimerization obtained with the $ReaxFF_{SiO}$ force field.

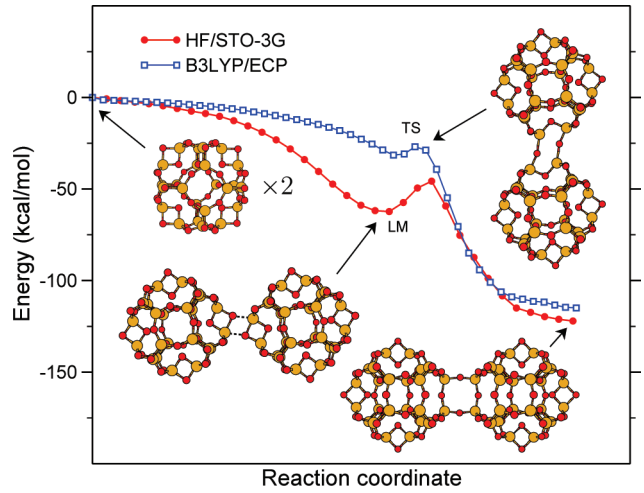

Figure 4. Reaction pathways for the $(SiO_2)_{24}$ dimerization obtained at the HF and DFT levels. The local minimum (LM) and transition state (TS) are emphasized.

The formation energy of the dimerized cages is −147.24 kcal/mol with the $ReaxFF_{SiO}$ force field, in very good agreement with the FB value.

III. Electronic Structure Calculations

The results obtained thus far with the FB pair potential and ReaxFF have been compared with calculations that treat the electronic structure explicitly. Two different approaches have been used for investigating the dimerization reaction involving monomer $(SiO_2)_{24}$ cages. Because of the relatively large number of atoms, we first limited our calculations to Hartree-Fock (HF) theory[34] with a minimal STO-3G[35] basis set to provide a rough estimate of the positions and energies of the low-lying stationary points on the potential energy surface (PES). We then refined these structures using density functional theory[36] and a larger basis set. For this purpose, the hybrid B3LYP functional[37] with a mixed double-ζ basis set (ECP-LANL2DZ[38] for silicon and 6-31G* for oxygen)[39] was chosen. The PES was surveyed using the Multi-Coordinate Driven Reaction Path Search program[40] (MCD v.1.2 by Imre Berente) combined with Gaussian03.[41]

Figure 4 shows the dimerization reaction profiles obtained with the HF/STO-3G and B3LYP/ECP approaches. In both cases the reaction exhibits a small local barrier for dimerization, with a transition state at least 25 kcal/mol lower in energy compared

to the two separated monomers. This finding suggests that the dimerization should be a favorable process, releasing the strain of the double-bridged Si_2O_2 rhombi of the $(SiO_2)_{24}$ cage, and that it should occur spontaneously under ambient conditions. The formation energies predicted by the two electronic structure calculations are −122.1 and −114.9 kcal/mol for the HF and DFT methods, respectively, in reasonable agreement with the results obtained in the previous section with the empirical approaches. The dimerization mechanisms are also similar to the $ReaxFF_{SiO}$ pathway of Figure 3, although the local minimum is barely stable in the DFT case. The rate-limiting step involves the double pivoting of the closest oxygen atoms of the two nanocages to form the siloxane bridges and is followed by the reorientation of the cages to stabilize these bridges.

The stable dimer obtained with both QM calculations differs slightly from the stable structures obtained with the empirical potentials, as the siloxane bridges are not in a common plane. In both the HF and DFT treatments the silica nanocages undergo a small rotation to increase their contact surface, lowering the symmetry from D_{2h} to C_{2v}. The C_{2v} dimer is also more stable with the $ReaxFF_{SiO}$ model but spontaneously rearranges into the D_{2h} structure with the FB potential. This result suggests that the Si−Si and O−O repulsions are probably too strong within the Flikkema−Bromley parametrization.

IV. Formation of More Complex Assemblies

As the $(SiO_2)_{24}$ cluster is reactive at room temperature due to the strain relaxation of the double-bridged Si_2O_2 units, the polymerization reaction should also occur under ambient conditions. Several ways of connecting the nanocages are illustrated in Figure 5, along with the corresponding formation energies for the FB model. A first important reaction is the formation of four additional siloxane bridges between the monomers, leading to the S_6 dimer shown in Figure 5a. This structure is about 220 kcal/mol more stable (FB potential) than the D_{2h} dimer previously considered, which is bound by only two siloxane bridges. A low-energy pathway for the formation of these additional bonds was determined using the doubly[32] nudged elastic band[33,34] method.

We were not able to locate simple paths connecting the doubly bridged D_{2h} or C_{2v} dimers to the 6-fold bound S_6 dimer. However, a reasonably short pathway was found involving a similar dimer bound by two siloxane bridges anchored on different silicons and lacking any particular symmetry. This dimer is shown as the starting point on the left of Figure 6 along with the entire pathway leading to the S_6 dimer structure. Dimerization into the 6-fold bonded structure is a multistep process, in which one, then two, and finally four extra siloxane bridges are formed successively. All the energy barriers are small, and no transition state exceeds the reference energy of the dissociated cages. This result suggests that the reaction pathway of Figure 6 would also be spontaneous under ambient conditions.

The high symmetry of the silica nanocage gives rise to various possible connections in larger assemblies. Two-dimensional arrays can be bound by double siloxane bridges, as shown for the four-cage example in Figure 5b. A three-dimensional packing deriving from this array can be built as well, still using only double siloxane bridges, leading to the octahedral motif depicted in Figure 5d. Alternatively, the T_d subgroup of the O_h group can be exploited by linking the nanocages with six siloxane bridges, leading to the tetrahedral assembly shown in Figure 5c. This structure should be much more flexible than other frameworks bound by double siloxane bridges.

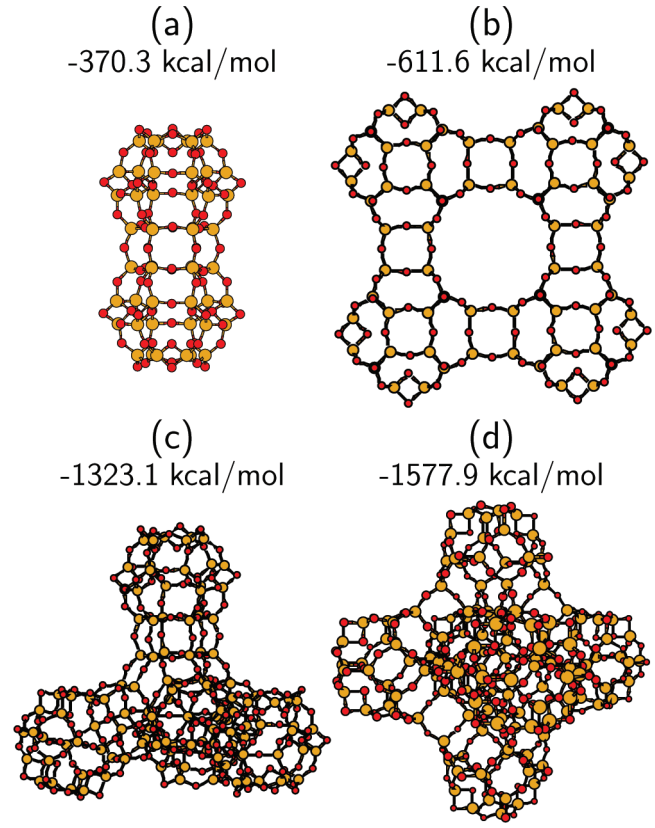

Figure 5. Fully coordinated assemblies of silica nanocages with (a) two units bound by six siloxane bridges, (b) four units bound by two siloxane bridges, (c) five units bound by six siloxane bridges in a tetrahedral configuration, and (d) six units bound by two siloxane bridges in an octahedral configuration. The binding energies relative to the isolated cages are given for the FB pair potential.

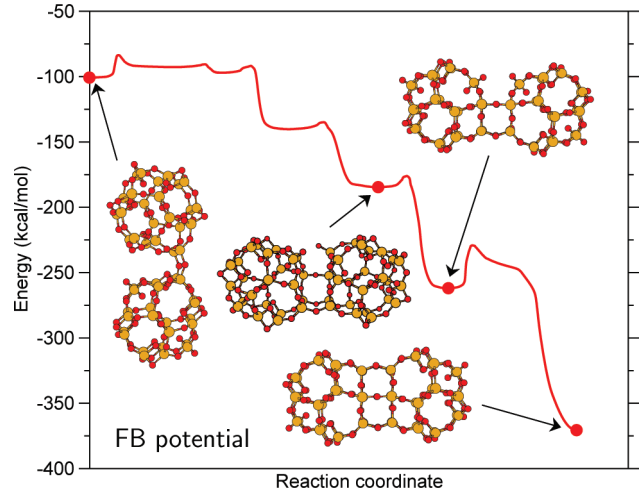

Figure 6. Reaction pathway for the formation of four additional siloxane bridges between two $(SiO_2)_{24}$ dimers, obtained with the FB pair potential. The energies are relative to the isolated nanocages.

Finally, we have tested the predicted high reactivity between silica nanocages by simulating the spontaneous evolution of several clusters under periodic boundary conditions within the $ReaxFF_{SiO}$ model. A molecular dynamics trajectory was initiated by placing eight cages in random locations and orientations inside a cubic box with an edge size of 35 Å, ensuring no initial overlap or connection between them. The corresponding density was 0.45 kg/dm^3. The ReaxFF simulations were performed using an NVT-ensemble with a time step of 0.25 fs and $T = 300$ K.

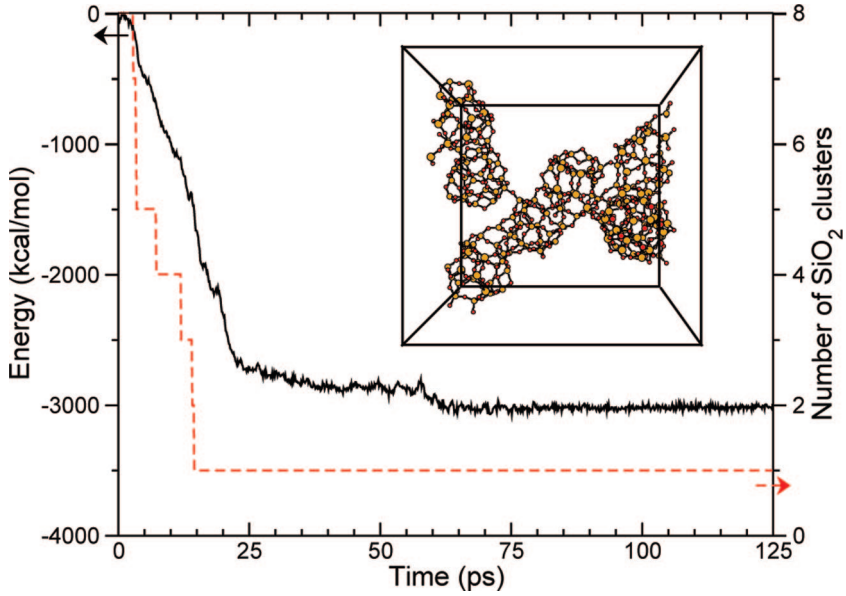

Figure 7. Self-assembly of eight $(SiO_2)_{24}$ nanocages obtained from molecular dynamics simulations with the $ReaxFF_{SiO}$ force field at 300 K. The solid black line and dashed red line show the time variations of the potential energy relative to the dissociated units and the instantaneous number of individual SiO_2 clusters, respectively. The inset shows the final configuration after 125 ps.

The temperature was controlled using a Berendsen thermostat with a temperature damping constant of 100 fs. The total simulation time was 125 ps (500000 iterations). During the simulation we monitored the number of remaining $(SiO_2)_{24}$ clusters using the ReaxFF bond orders as a connectivity criterion; any clusters bound together with a bond order of 0.3 or less were considered separate molecules. A ReaxFF bond order of 0.3 roughly equates for the Si−O pair to a distance of 2.3 Å. The time variations of the configurational energy obtained during this trajectory are shown in Figure 7, along with the number of connected SiO_2 clusters. The eight nanocages quickly react with each other and self-assemble into a single connected silica framework in about 15 ps. The resulting structure remains in a nearly stationary state for the rest of the simulation. Inspecting this final structure (see inset of Figure 7) reveals that the cages are bound together by only one or two siloxane bridges and that they are not yet able to arrange themselves into the highly symmetric patterns shown in Figure 5. We expect the formation of these compact networks to require much longer times, partly due to the cooperative motion that is expected for such complex, multicage and multistep processes.

V. Discussion and Conclusion

A common feature of all dimerization processes between silica nanocages is the high reactivity of the double-bridge Si_2O_2 rhombi. These units are progressively eliminated as the polymerization continues. As a result, only the surface of the growing material remains reactive. As the emerging structure becomes larger, it thus approaches more and more the features of a chemically inert material. Moreover, the addition of each $(SiO_2)_{24}$ nanocage decreases the total binding energy of the polymerizing structure considerably (by about 150 kcal/mol), yielding an ever more stable structure that can, for instance, withstand considerably higher temperatures than the monomer nanocage discussed above.

These properties could be suitable for the creation of adhesives and protective coatings. Due to its dielectric character, the polymerized $(SiO_2)_{24}$ units may be useful for manufacturing nanoscale capacitors in miniature electronic devices, which should be operational over a broad temperature range. Due to its high porosity and its high surface area, the material might also be suitable for use in chromatography columns, or as a substrate for heterogeneous catalysis. Finally, due to the periodicity of the nanocages, the $(SiO_2)_{24}$-based solid might be employed as a storage matrix for small metal clusters and thus find application as a three-dimensional photonic crystal for X-rays.[44] Since the polymerized $(SiO_2)_{24}$ should be chemically inert, such devices could work in a wide range of environments.

A natural extension of the present work would be to study the interactions of the nanocages and their assemblies with water. The H_2O molecule can drastically alter the properties of silica and is particularly active in weakening the Si−O bond.[45,46] The presence of water molecules around the silica clusters could facilitate dimerization through a catalytic process but might also destabilize the individual cage structures or the siloxane bridges. The water-mediated interaction between silica clusters could be conveniently studied using the same QM approaches or, following Du and co-workers,[47] using a QM/MM method. At the level of force fields, $ReaxFF_{SiO}$ or the recent potential developed in the Payne group[48] could be employed to perform large-scale explicit molecular simulations of hydrolyzed silica clusters.

To summarize, we have explored the stability of fully coordinated octahedral $(SiO_2)_{24}$ nanocages toward coalescence using a variety of theoretical methods. Molecular dynamics simulations performed with explicit pair potentials and the Reax force field show a spontaneous dimerization in which the two monomers bind to each other by two siloxane bridges. The pathway for this reaction appears to be essentially barrierless and exothermic by about 150 kcal/mol. Our quantum chemical calculations at both Hartree-Fock and density functional theory levels lead to the same findings, suggesting that dimerization should occur under ambient conditions.

Several possible ways of connecting SiO_2 nanocages have been proposed, based on the high symmetry of the octahedral monomer. These early stages of self-assembly all proceed by siloxane bridging, and even the formation of six such bridges involves only moderate energy barriers. Different two- and three-dimensional packings of silica nanocages can be considered depending on the number of siloxane connections. Finally, we

have speculated about potential applications of the polymerized $(SiO_2)_{24}$ nanocages in various fields such as chemistry, electronics, and optics.

Acknowledgment. N.N. is the recipient of a PhD studentship from the "Ministère de l'Enseignement Supérieur et de la Recherche". A part of this work was financed by the EADS Corporate Foundation. We like to thank the "Institut du Développement et des Ressources en Informatique Scientifique" (IDRIS), who supported part of the computational work discussed herein. The authors are also grateful to Dr. Roberto Santoprete for his help during the early stages of this work and to Dr. Grygoriy Dolgonos for his technical assistance.

Supporting Information Available: Animation of the spontaneous dimerization of two silica nanocages simulated with the Flikkema−Bromley pair potential (mpg format). This material is available free of charge via the Internet at http://pubs.acs.org.

References and Notes

(1) (a) *The Physics and Chemistry of SiO2 and the Si−SiO2 interface*; Helms, C. R., Deal, B. E., Eds.; Plenum Press: New York, 1988. (b) *The Surface Properties of Silica*; Legrand, A. P., Ed.; Wiley: New York, 1998.
(2) Muller, D. A.; Sorsch, T.; Moccio, S.; Baumann, F. H.; Evans-Lutterodt, K.; Timp, G. *Nature* **1999**, *399*, 758.
(3) Suzuki, K.; Ikari, K.; Imai, H. *J. Am. Chem. Soc.* **2004**, *126*, 462.
(4) Tan, W.; Wang, K.; He, X.; Zhao, X. J.; Drake, T.; Wang, L.; Bagwe, R. P. *Med. Res. Rev.* **2004**, *24*, 621.
(5) Gole, J. L. *Nano Lett.* **2001**, *1*, 449.
(6) Bromley, S. T. *Nano Lett.* **2004**, *4*, 1427.
(7) Song, J.; Choi, M. *Phys. Rev. B* **2002**, *65*, 241302.
(8) Bromley, S. T. *Cryst. Eng. Commun.* **2007**, *9*, 463.
(9) Harkless, J. A. W.; Stillinger, D. K.; Stillinger, F. H. *J. Phys. Chem.* **1996**, *100*, 1098.
(10) Nayak, S. K.; Rao, B. K.; Khanna, S. N.; Jena, P. *J. Chem. Phys.* **1998**, *109*, 1245.
(11) Chelikowsky, J. R. *Phys. Rev. B* **1998**, *57*, 3333.
(12) Nedelec, J. M.; Hench, L. L. *J. Non-Cryst. Solids* **2000**, *277*, 106.
(13) Bromley, S. T.; Zwijnenburg, M. A.; Maschmeyer, T. *Phys. Rev. Lett.* **2003**, *90*, 035502.
(14) Lu, W. C.; Wang, C. Z.; Nguyen, V.; Schmidt, M. W.; Gordon, M. S.; Ho, K. M. *J. Phys. Chem. A* **2003**, *107*, 6936.
(15) Sun, Q.; Wang, Q.; Jena, P. *Phys. Rev. Lett.* **2004**, *92*, 039601.
(16) Bromley, S. T.; Zwijnenburg, M. A.; Maschmeyer, T. *Phys. Rev. Lett.* **2004**, *92*, 039602.
(17) Zwijnenburg, M. A.; Bromley, S. T.; Flikkema, E.; Maschmeyer, T. *Chem. Phys. Lett.* **2004**, *385*, 389.
(18) Zhang, D. J.; Zhao, M. W.; Zhang, R. Q. *J. Phys. Chem. B* **2004**, *108*, 18451.
(19) Bromley, S. T.; Flikkema, E. *Phys. Rev. Lett.* **2005**, *95*, 185505.
(20) Bromley, S. T.; Flikkema, E. *Comput. Mater. Sci.* **2006**, *35*, 382.
(21) Zhang, D.; Wu, J.; Zhang, R. Q.; Lio, C. *J. Phys. Chem. B* **2006**, *110*, 17757.
(22) Wojdel, J. C.; Zwijnenburg, M. A.; Bromley, S. T. *Chem. Mater.* **2006**, *18*, 1464.
(23) He, Y.; Cao, C.; Wan, Y. X.; Cheng, H.-P. *J. Chem. Phys.* **2006**, *124*, 024722.
(24) Muralidharan, K.; Cao, C.; Wan, Y.-X.; Runge, K.; Cheng, H.-P. *Chem. Phys. Lett.* **2007**, *437*, 92.
(25) Tsuneyuki, S.; Tsukada, M.; Aoki, H.; Matsui, Y. *Phys. Rev. Lett.* **1988**, *61*, 869.
(26) Schweigert, I. V.; Lehtinen, K. E.; Carrier, M. J.; Zachariah, M. R. *Phys. Rev. B* **2002**, *65*, 235410.
(27) Flikkema, E.; Bromley, S. T. *Chem. Phys. Lett.* **2003**, *378*, 622.
(28) Van Duin, A. C. T.; Dasgupta, S.; Lorant, F.; Goddard, W. A. *J. Phys. Chem. A* **2001**, *105*, 9396.
(29) Van Duin, A. C. T.; Strachan, A.; Stewman, S.; Zhang, Q. S.; Xu, X.; Goddard, W. A. *J. Phys. Chem. A* **2003**, *107*, 3803.
(30) LaViolette, R. A.; Benson, M. T. *J. Chem. Phys.* **2000**, *112*, 9269.
(31) Van Beest, B. W. H.; Kramer, G. J.; van Santeen, R. A. *Phys. Rev. Lett.* **1990**, *64*, 1955.
(32) Trygubenko, S. A.; Wales, D. J. *J. Chem. Phys.* **2004**, *120*, 2082.
(33) Wales, D. J. *OPTIM: A program for Optimising Geometries and Calculating Reaction Pathways*, University of Cambridge.
(34) Roothan, C. C. J. *Rev. Mod. Phys.* **1951**, *23*, 69.
(35) (a) Hehre, W. J.; Stewart, R. F.; Pople, J. A. *J. Chem. Phys.* **1969**, *51*, 2657. (b) Hehre, W. J.; Ditchfield, R.; Stewart, R. F.; Pople, J. A. *J. Chem. Phys.* **1970**, *52*, 2769.
(36) Hohenberg, P.; Kohn, W. *Phys. Rev.* **1964**, *136*, B864.
(37) (a) Becke, A. D. *Phys. Rev. A* **1988**, *38*, 3098. (b) Lee, C.; Yang, W.; Parr, R. G. *Phys. Rev. B* **1988**, *37*, 785. (c) Stephens, P. J.; Devlin, F. J.; Chabalowski, C. F.; Frisch, M. J. *J. Phys. Chem.* **1994**, *98*, 11623.
(38) Hay, P. J.; Wadt, W. R. *J. Chem. Phys.* **1985**, *82*, 284.
(39) Hehre, W. J.; Ditchfield, R.; Pople, J. A. *J. Chem. Phys.* **1972**, *56*, 2257.
(40) Berente, I.; Naray-Szabo, G. J. *J. Phys. Chem. A* **2006**, *110*, 772.
(41) Frisch, M. J. ; Trucks, G. W.; Schlegel, H. B.; Scuseria, G. E.; Robb, M. A.; Cheeseman, J. R.; Montgomery Jr., J. A.; Vreven, T.; Kudin, K. N.; Burant, J. C.; Millam, J. M.; Iyengar, S. S.; Tomasi, J.; Barone, V.; Mnnucci, B.; Cossi, M.; Scalmani, G.; Rega, N.; Petersson, G. A.; Nakatsuji, H.; Hada, M.; Ehara, M.; Toyota, K.; Fukuda, R.; Hasegawa, J.; Ishida, M.; Nakajima, T.; Honda, O.; Kitao, H.; Nakai, H.; Klene, M.; Li, X.; Knox, J. E.; Hratchian, H. P.; Cross, J. B.; Bakken, V.; Adamo, C.; Jaramillo, J.; Gomperts, R.; Stratmann, R. E.; Yazyev, O.; Austin, A. J.; Cammi, R.; Pomelli, C.; Ochterski, J. W.; Ayala, P. Y.; Morokuma, K.; Voth, G. A.; Salvador, P.; Dannenberg, J. J.; Zakrzewski, V. G.; Dapprich, S.; Daniels, A. D.; Strain, M. C.; Farkas, O.; Malick, D. K.; Rabuck, A. D.; Raghavachari, K.; Foresman, J. B.; Ortiz, J. V.; Cui, Q.; Baboul, A. G.; Clifford, S.; Cioslowski, J.; Stefanov, B. B.; Liu, G.; Liashenko, A.; Piskorz, P.; Komaromi, I.; Martin, R. L.; Fox, D. J.; Keith, T.; Al-Laham, M. A.; Peng, C. Y.; Nanayakkara, A.; Challacombe, M.; Gill, P. M. W.; Johnson, B.; Chen, W.; Wong, M. W.; Gonzalez, C.; Pople, J. A. *Gaussian 03 (Revision C.02)*, Gaussian Inc.: Wallingford, CT, 2004.
(42) Henkelman, G.; Jónsson, H. *J. Chem. Phys.* **1999**, *111*, 7010.
(43) Henkelman, G.; Uberuaga, B. P.; Jónsson, H. *J. Chem. Phys.* **2000**, *113*, 9901.
(44) Pevtsov, A. B.; Kurdyukov, D. A.; Golubev, V. G.; Akimov, A. V.; Meluchev, A. A.; Sel'kin, A. V.; Kaplyanskii, A. A.; Yakovlev, D. R.; Bayer, M. *Phys. Rev. B* **2007**, *75*, 153101.
(45) Stolen, R. H.; Walrafen, G. E. *J. Chem. Phys.* **1976**, *64*, 2623.
(46) Tripp, C. P.; Hair, M. L. *Langmuir* **1992**, *8*, 1120.
(47) Du, M.-H.; Kolchin, A.; Cheng, H.-P. *J. Chem. Phys.* **2004**, *120*, 1044.
(48) Cole, D. J.; Payne, M. C.; Csányu, G.; Spearing, S. M.; Ciacchi, L. C. *J. Chem. Phys.* **2007**, *127*, 204704.

JP804528Z